Molecular Dynamics

DOI: 10.1002/anie.201310237

Competition Between Concerted and Stepwise Dynamics in the Triplet Di-π-Methane Rearrangement**

*Gonzalo Jiménez-Osés, Peng Liu, Ricardo A. Matute, and Kendall N. Houk**

Dedicated to the MPI für Kohlenforschung on the occasion of its centenary

Abstract: *The molecular dynamics of the triplet-state Zimmerman di-π-methane rearrangement of dibenzobarrelene were computed with B3LYP and M06-2X density functionals. All productive quasiclassical trajectories involve sequential formation and cleavage of C–C bonds and an intermediate with lifetimes ranging from 13 to 1160 fs. Both dynamically concerted and stepwise trajectories are found. The average lifetime of this intermediate is significantly shorter than predicted by either transition-state theory or the Rice–Ramsperger–Kassel–Marcus model, thus indicating the non-statistical nature of the reaction mechanism.*

Theoretical studies of photochemical reaction dynamics have emphasized the role of surface crossings and conical intersections on singlet surfaces.[1] There are fewer explorations of reaction dynamics on triplet surfaces.[2] In a recent report, we described the triplet potential energy surface (PES) of the Zimmerman di-π-methane rearrangement (DPM) of dibenzobarrelene (DBB; Scheme 1 and Figure S1 in the Supporting Information).[3] Based on the topology of the triplet surface of this reaction, we have suggested that the DPM rearrangement of DBB could proceed by competing one-step and two-step pathways;[3] this has long been a point of mechanistic interest about this reaction.

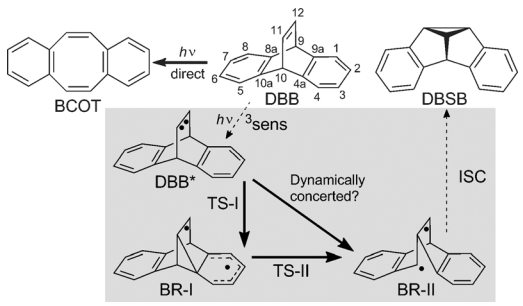

Scheme 1. Reaction mechanism for the Zimmerman di-π-methane rearrangement of dibenzobarrelene.

Transition-state theory (TST)[4] and the Rice–Ramsperger–Kassel–Marcus (RRKM) model[5] are based on the redistribution of internal energy among the available vibrations and internal rotations of a molecule (IVR) occurring more rapidly than bond-forming or bond-breaking events.[6] However, as shown in pioneering studies by Carpenter et al.,[7] nonstatistical dynamics affecting the rate and selectivity occur for reactions on surfaces containing a shallow intermediate with excess total energy, which is the case for the DPM rearrangement on the triplet surface. Such nonstatistical reaction dynamics have been reviewed in detail.[7b,c] Molecular dynamics studies by Reyes and Carpenter, and Hase and co-workers, as well as others have demonstrated the critical role of nonstatistical effects in reactions involving singlet biradicals,[7a,8] radical cations,[9] and carbenes.[10] Singleton and co-workers have described nonstatistical pathways in alkene hydroborations,[11] Diels–Alder reactions,[12] and enyne–allene cyclizations.[13] We have also described the dynamics of singlet carbene cycloadditions.[14]

Triplet photosensitization of bicyclic dienes or aromatics such as DBB leads to bullvalene or dibenzosemibullvalene (DBSB) derivatives by Zimmerman's DPM rearrangement,[15] whereas the excited singlet pathway yields cyclooctatetraene derivatives (BCOT; Scheme 1).[16] A three-dimensional representation of the triplet surface and the minimum-energy pathway calculated for this reaction by three different methods, are represented in Figure S1. The triplet excited dibenzobarrelene DBB* must overcome the barrier associated with phenyl-vinyl bridging (TS-I) to yield the 1,4-diradical BR-I. A second barrier, TS-II, leads to the 1,3-diradical BR-II, which is the most stable species on the triplet surface. From BR-II, the reaction enters the radiationless decay channel and intersystem-crosses (ISC) to form DBSB as the final product in the ground singlet state. The surface could also be traversed directly via TS-III (Figure S1). However, this pathway is not accessible because of its very high energy.

As shown in Figure S1A, the barrier calculated for TS-I is the highest energy point along the minimum energy pathway and determines the rate of the reaction. The intermediate BR-I is a shallow minimum on the PES and the barrier for the second step (TS-II) is small (< 2 kcal mol^{-1}). Therefore, DBB* may reach BR-II directly through a one-step mecha-

[*] Dr. G. Jiménez-Osés, Dr. P. Liu, Dr. R. A. Matute, Prof. Dr. K. N. Houk
Department of Chemistry and Biochemistry
University of California, Los Angeles
607 Charles E. Young Drive East, Los Angeles, CA 90095-1569 (USA)
E-mail: houk@chem.ucla.edu

[**] This research was supported by the National Science Foundation (CHE-1059084). Calculations were performed on the Hoffman2 and Dawson2 GPU clusters at UCLA and the Extreme Science and Engineering Discovery Environment (XSEDE), which is supported by the National Science Foundation (OCI-1053575).

Supporting information for this article is available on the WWW under http://dx.doi.org/10.1002/anie.201310237.

nism, since the intermediate BR-I is formed with excess energy after passing the first barrier, and dynamical effects could facilitate the transition over the very small second barrier, thus making the whole process dynamically concerted.

To characterize the dynamics of this photochemical reaction, we explored it with quasiclassical dynamics.[17] Both B3LYP and M06-2X methods were used, but only the B3LYP results will be discussed here since energies calculated at this level are closer to the CASMP2 reference values (see the Supporting Information for computational methods). Solvent effects were not included in the simulations because the optimization of the relevant stationary points in the experimental solvents (toluene or benzene) showed a negligible influence in both the energies and geometries (see Table S1).

The trajectories were initialized from normal mode sampling of TS-I (Figure 1 A) to approximate a quantum mechanical Boltzmann distribution of the vibrational levels at 298 K. The overlay of the sampled TS-I geometries (Figure 1 B) shows the variation in length of the forming C11–C4a

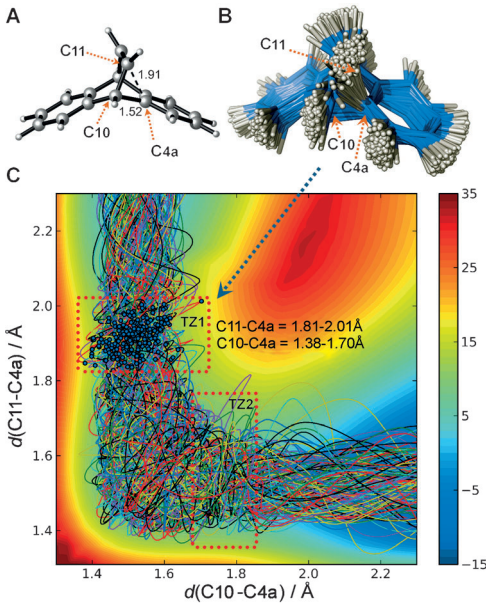

Figure 1. A) Optimized structure of TS-I (transition structure). B) Ensemble of sampled geometries of TS-I used as starting structures for the simulations (transition state). C) Trajectories on the triplet potential energy surface (contour diagram, energies in kcal mol^{-1}) for the Zimmerman DPM rearrangement of DBB. All calculations were performed at the B3LYP/6-31G(d) level.

bond in this transition state. Significant distortion of the C10–C4a bond, which is broken in the second transition state TS-II, occurs at the sampled geometries of TS-I. However, the bond stretching of C10–C4a in these starting geometries does not correlate with the lifetimes of the intermediates derived from them, as described later.

Of 256 trajectories, 241 (94 %) were productive within the simulation time limit of 1500 fs, thus connecting reactant DBB* and BR-II, the triplet species which undergoes ISC and coupling to form the ground-state rearranged product. The productive trajectories along the reaction coordinate on the triplet surface are mapped onto a contour energy diagram in Figure 1 C. All trajectories show the sequential process of formation of the C11–C4a bond followed by cleavage of the C10–C4a bond.

For analysis purposes, we defined the transition zones for TS-I (TZ1) and TS-II (TZ2) to delimit the two high-energy regions which are traversed throughout the reaction (Figure 2)[18,19] The lifetime of the intermediate (t_{life}), is thus

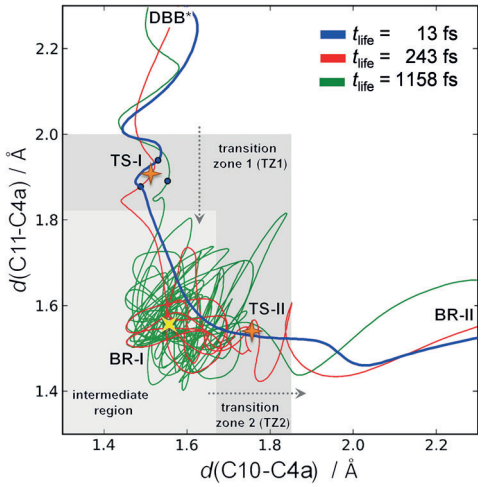

Figure 2. Representative B3LYP/6-31G(d) trajectories for the dynamically concerted (in blue), intermediate (in red), and stepwise (in green) pathways of the DPM rearrangement. Intermediate lifetimes (t_{life}) are displayed for each trajectory. Stationary points in the PES are displayed as yellow (minimum) and orange (TS) stars.

defined as the time between departure from TZ1 and entrance into TZ2, and has the average value of (233 ± 188) fs. The average time to traverse TZ1 is (27 ± 14) fs and the time to traverse TZ2 is (19 ± 11) fs. These values are similar to those determined by Nummela and Carpenter for methyl loss from the acetone radical cation, a reaction with strong nonstatistical dynamics.[20]

Recrossing trajectories were neglected in the above analysis since of the 256 trajectories, only seven recrossed in the backward direction (reactant to reactant) and only eight trajectories recrossed in the forward direction (product to product). There were two trajectories that escaped from the BR-I intermediate after multiple vibrations (maximum t_{life} = 643 fs) and returned to reactant by passing through TS-I again.

All the productive trajectories ended at BR-II, but they differ in the way they traverse the shallow well of the BR-I intermediate. A time of 60 fs is typical for the stretching vibration of a C–C bond. Therefore, trajectories with a lifetime of BR-I below 60 fs can be considered to follow a dynamically concerted pathway from TS-I to BR-II, whereas those with a lifetime of BR-I above that value are indicative of a dynamically stepwise pathway. Figure 2 shows an individual trajectory (in red) for a typical two-step

pathway, where the C11–C4a is formed first to give the BR-I geometry, and then spends some time vibrating before the cleavage of the C10–C4a bond occurs. The lifetime of intermediate BR-I is 243 fs in this trajectory, which involves at least four C–C vibrations prior to bond cleavage. Although rare, very long trajectories of about 1 ps were also observed, which is consistent with stepwise mechanisms (Figure 2 in green). Figure 2 also shows an individual trajectory (in blue) for the direct one-step pathway, where the C11–C4a bond formation and the C10–C4a bond dissociation are concerted. In this case the intermediate has an exceedingly short lifetime of 13 fs, which is much shorter than the 60 fs threshold described before. A total of 24 trajectories (10% of the productive ones; Figure 3B) were below this limit, thus

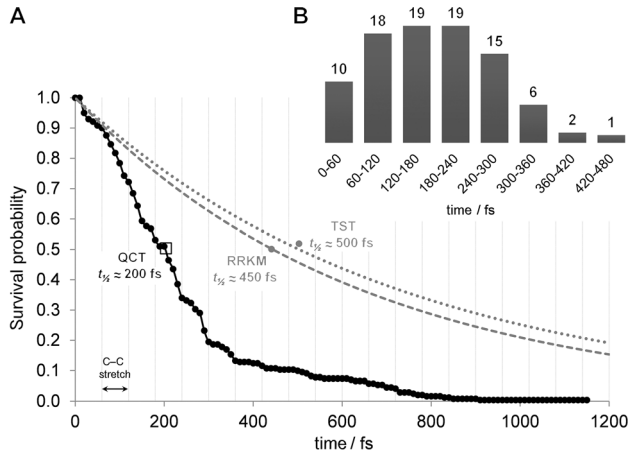

Figure 3. A) The survival probability (P) of the intermediate BR-I derived from quasiclassical trajectories (QTC) is shown in black. Monoexponential first-order decays ($P = e^{-kt}$) simulated from the classical rate constants obtained through TST ($k = 1.38 \times 10^{-3}$ fs^{-1}) and RRKM ($k = 1.56 \times 10^{-3}$ fs^{-1}) theories, are shown in grey. All curves were obtained at the B3LYP/6-31G(d) level. B) Distribution of intermediate BR-I lifetimes: each column represents the percentage of productive trajectories that have entered TZ2, at intervals of approximately one C–C vibration (ca. 60 fs).

reflecting the non-negligible dynamically concerted character of this reaction. However, none of the direct trajectories skipped the intermediate (BR-I) region on the PES. That is, stretching of the C10–C4a bond to the TS-II distance (ca. 1.8 Å) always occurs *after* the first C11–C4a bond has already fully formed. This result confirms that there are no alternative pathways for the concerted reaction in terms of geometry.

Figure 3A shows the survival probability of BR-I, measured as the time required for transforming TZ1 into TZ2 (i.e., the intermediate lifetime). After a short nondecaying period corresponding to the minimum time necessary to cleave the C10–C4a bond (ca. 10 fs), the distribution shows a fast decay resulting from strong coupling of the vibrational modes with the reaction coordinate, followed by a slow decay in which trajectories follow the classical behavior because of IVR. A single population with a characteristic half-life[20] could not be accurately described, and the natural logarithmic representation of these data[21] did not show the linear behavior typical of unimolecular reactions (see Figure 3A, curves in greay, and Figure S5). This multiphasic profile does not fit to biexponential decays[14] either. This significant deviation from classical kinetic models reveals the impact of nonstatistical dynamics on the DPM rearrangement. A similar behavior was described for the retinal chromophore.[22] The half-life of intermediate BR-I (ca. 200 fs) is much less than the values calculated from the statistical TST or RRKM theories (ca. 500 and 450 fs, respectively; see Table S2). Moreover, most of the trajectories fall in a nonstatistical regime: at the RRKM half-life time, 89% of the productive B3LYP trajectories already reached the BR-II region (see Figure S5 for results with M06-2X functional).

The origins of nonstatistical behavior have been discussed. For instance, Carpenter and co-workers use the term dynamic matching for the vibrational coupling of the entrance channel to the exit channel of an intermediate.[23] Mode-specific chemical activation, in which the excess of kinetic energy is accumulated preferentially in specific vibrational modes, has been proposed as the source of nonstatistical effects in deazetization reactions,[7b,24] which show energy profiles very similar to the one calculated for the DPM rearrangement. In the reaction studied here, no evidence for mode specificity has been found, presumably because of the high structural complexity and the mixed character of the vibrations calculated for the intermediate structures.

In summary, quasiclassical trajectories calculations indicate that the Zimmerman di-π-methane rearrangement of dibenzobarrelene involves both dynamically concerted short trajectories (< 60 fs), and dynamically stepwise trajectories where intermediates exhibit lifetimes predicted by the statistical TST and RRKM models. The observed nonstatistical effects are due to nonspecific chemical activation proposed analogously for cyclopropanation[25] and hydroboration[11] reactions. However, irrespective of the time required to complete each reactive trajectory, the region of the cyclopropane intermediate is always sampled. Although dynamically concerted, the reaction is bonding stepwise[26] in that bond making and bond breaking occur sequentially in a time shorter than a vibration.

Received: November 25, 2013
Published online: March 11, 2014

Keywords: density functional calculations · molecular dynamics · photochemistry · rearrangement · statistical mechanics

[1] B. G. Levine, T. J. Martínez, *Annu. Rev. Phys. Chem.* **2007**, *58*, 613–634.
[2] a) J. D. Gezelter, W. H. Miller, *J. Chem. Phys.* **1996**, *104*, 3546–3554; b) H. Tachikawa, *J. Organomet. Chem.* **1998**, *555*, 161–166; c) S. Mai, P. Marquetand, L. Gonzalez, *arXiv:1302.1438 [physics.chem-ph]* **2013**.
[3] R. A. Matute, K. N. Houk, *Angew. Chem.* **2012**, *124*, 13274–13277; *Angew. Chem. Int. Ed.* **2012**, *51*, 13097–13100.
[4] D. G. Truhlar, B. C. Garrett, S. J. Klippenstein, *J. Phys. Chem.* **1996**, *100*, 12771–12800.

[5] a) L. S. Kassel, *Chem. Rev.* **1932**, *10*, 11 – 25; b) O. K. Rice, H. C. Ramsperger, *J. Am. Chem. Soc.* **1927**, *49*, 1617 – 1629; c) R. A. Marcus, *J. Chem. Phys.* **1952**, *20*, 352 – 354; d) R. A. Marcus, *J. Chem. Phys.* **1952**, *20*, 355 – 359.
[6] J. I. Steinfeld, J. S. Francisco, W. L. Hase, *Chemical Kinetics and Dynamics*, 2nd ed., Prentice Hall, Upper Saddle River, NJ, **1998**.
[7] a) M. B. Reyes, B. K. Carpenter, *J. Am. Chem. Soc.* **2000**, *122*, 10163 – 10176; b) B. K. Carpenter, *Annu. Rev. Phys. Chem.* **2005**, *56*, 57 – 89; c) B. K. Carpenter, *Chem. Rev.* **2013**, *113*, 7265 – 7286.
[8] a) C. Doubleday, G. Li, W. L. Hase, *Phys. Chem. Chem. Phys.* **2002**, *4*, 304 – 312; b) D. A. Singleton, C. Hang, M. J. Szymanski, M. P. Meyer, A. G. Leach, K. T. Kuwata, J. S. Chen, A. Greer, C. S. Foote, K. N. Houk, *J. Am. Chem. Soc.* **2003**, *125*, 1319 – 1328; c) C. Doubleday, C. P. Suhrada, K. N. Houk, *J. Am. Chem. Soc.* **2006**, *128*, 90 – 94; d) M. Schmittel, C. Vavilala, R. Jaquet, *Angew. Chem.* **2007**, *119*, 7036 – 7039; *Angew. Chem. Int. Ed.* **2007**, *46*, 6911 – 6914; e) M. Hamaguchi, M. Nakaishi, T. Nagai, T. Nakamura, M. Abe, *J. Am. Chem. Soc.* **2007**, *129*, 12981 – 12988.
[9] A. Bach, J. M. Hostettler, P. Chen, *J. Chem. Phys.* **2006**, *125*, 024304.
[10] A. E. Litovitz, I. Keresztes, B. K. Carpenter, *J. Am. Chem. Soc.* **2008**, *130*, 12085 – 12094.
[11] Y. Oyola, D. A. Singleton, *J. Am. Chem. Soc.* **2009**, *131*, 3130 – 3131.
[12] Z. Wang, J. S. Hirschi, D. A. Singleton, *Angew. Chem.* **2009**, *121*, 9320 – 9323; *Angew. Chem. Int. Ed.* **2009**, *48*, 9156 – 9159.
[13] T. Bekele, C. F. Christian, M. A. Lipton, D. A. Singleton, *J. Am. Chem. Soc.* **2005**, *127*, 9216 – 9223.
[14] L. Xu, C. E. Doubleday, K. N. Houk, *J. Am. Chem. Soc.* **2011**, *133*, 17848 – 17854.
[15] a) H. E. Zimmerman, G. L. Grunewald, *J. Am. Chem. Soc.* **1966**, *88*, 183 – 184; b) E. Ciganek, *J. Am. Chem. Soc.* **1966**, *88*, 2882 – 2883; c) H. E. Zimmerman, R. W. Binkley, R. S. Givens, M. A. Sherwin, *J. Am. Chem. Soc.* **1967**, *89*, 3932 – 3933.
[16] M. Reguero, F. Bernardi, H. Jones, M. Olivucci, I. N. Ragazos, M. A. Robb, *J. Am. Chem. Soc.* **1993**, *115*, 2073 – 2074.
[17] a) L. Xu, C. E. Doubleday, K. N. Houk, *J. Am. Chem. Soc.* **2010**, *132*, 3029 – 3037; b) L. Xu, C. E. Doubleday, K. N. Houk, *Angew. Chem.* **2009**, *121*, 2784 – 2786; *Angew. Chem. Int. Ed.* **2009**, *48*, 2746 – 2748; c) C. Doubleday, K. Bolton, W. L. Hase, *J. Phys. Chem. A* **1998**, *102*, 3648 – 3658.
[18] Transition zone for TS-I (TZ1) was defined as the subset of sampled C11–C14a bond lengths with a deviation below the 98th percentile of the bond length at the saddle point of TS-I. Similarly, the transition zone for TS-II (TZ2) was defined as the geometries deviated below the 98th percentile with respect to the broken C10–C14a bond at the saddle point of TS-II. The values derived from the productive trajectories for TZ1 and TZ2 at 298 K are (1.91 ± 0.09) Å for the forming C11–C4a bond and (1.76 ± 0.09) Å for the breaking C10–C4a bond, respectively.
[19] K. Black, P. Liu, L. Xu, C. Doubleday, K. N. Houk *Proc. Natl. Acad. Sci. USA* **2012**, *109*, 12860 – 12865.
[20] J. A. Nummela, B. K. Carpenter, *J. Am. Chem. Soc.* **2002**, *124*, 8512 – 8513.
[21] L. Yang, R. Sun, W. L. Hase, *J. Chem. Theory Comput.* **2011**, *7*, 3478 – 3483.
[22] M. Olivucci, A. Lami, F. Santoro, *Angew. Chem.* **2005**, *117*, 5248 – 5251; *Angew. Chem. Int. Ed.* **2005**, *44*, 5118 – 5121.
[23] a) B. K. Carpenter, *J. Am. Chem. Soc.* **1995**, *117*, 6336 – 6344; b) L. M. Goldman, D. R. Glowacki, B. K. Carpenter, *J. Am. Chem. Soc.* **2011**, *133*, 5312 – 5318.
[24] a) B. K. Carpenter, *J. Phys. Org. Chem.* **2003**, *16*, 858 – 868; b) B. K. Carpenter, *Angew. Chem.* **1998**, *110*, 3532 – 3543; *Angew. Chem. Int. Ed.* **1998**, *37*, 3340 – 3350.
[25] B. K. Carpenter, J. Pittner, L. Veis, *J. Phys. Chem. A* **2009**, *113*, 10557 – 10563.
[26] a) P. A. Leber, J. E. Baldwin, *Acc. Chem. Res.* **2002**, *35*, 279 – 287; b) J. E. Baldwin, *Chem. Rev.* **2003**, *103*, 1197 – 1212.

